Designing Cost-Effective Biopharmaceutical Facilities Using Mixed-Integer Optimization

Songsong Liu
Centre for Process Systems Engineering, Dept. of Chemical Engineering, University College London, Torrington Place, London WC1E 7JE, U.K.

Ana S. Simaria and Suzanne S. Farid
The Advanced Centre for Biochemical Engineering, Dept. of Biochemical Engineering, University College London, Torrington Place, London WC1E 7JE, U.K.

Lazaros G. Papageorgiou
Centre for Process Systems Engineering, Dept. of Chemical Engineering, University College London, Torrington Place, London WC1E 7JE, U.K.

DOI 10.1002/btpr.1795
Published online October 3, 2013 in Wiley Online Library (wileyonlinelibrary.com)

Chromatography operations are identified as critical steps in a monoclonal antibody (mAb) purification process and can represent a significant proportion of the purification material costs. This becomes even more critical with increasing product titers that result in higher mass loads onto chromatography columns, potentially causing capacity bottlenecks. In this work, a mixed-integer nonlinear programming (MINLP) model was created and applied to an industrially relevant case study to optimize the design of a facility by determining the most cost-effective chromatography equipment sizing strategies for the production of mAbs. Furthermore, the model was extended to evaluate the ability of a fixed facility to cope with higher product titers up to 15 g/L. Examination of the characteristics of the optimal chromatography sizing strategies across different titer values enabled the identification of the maximum titer that the facility could handle using a sequence of single column chromatography steps as well as multi-column steps. The critical titer levels for different ratios of upstream to dowstream trains where multiple parallel columns per step resulted in the removal of facility bottlenecks were identified. Different facility configurations in terms of number of upstream trains were considered and the trade-off between their cost and ability to handle higher titers was analyzed. The case study insights demonstrate that the proposed modeling approach, combining MINLP models with visualization tools, is a valuable decision-support tool for the design of cost-effective facility configurations and to aid facility fit decisions. © 2013 The Authors. Published by Wiley Periodicals, Inc. on behalf of American Institute of Chemical Engineers *Biotechnol. Prog.*, 29:1472–1483, 2013
Keywords: biopharmaceutical facility design, monoclonal antibody purification, chromatography, mixed integer non-linear programming, antibody titers

Introduction

As the monoclonal antibody (mAb) sector has matured, it has become critical to rapidly identify the most cost-effective purification processes that can handle increasing upstream productivities in a timely manner and overcome existing purification bottlenecks.[1–3] Chromatography operations are identified as critical steps in a mAb purification process and can represent a significant proportion of the purification material costs, particularly due to the use of expensive affinity matrices as well as the high amounts of buffer reagents required. Higher product titers allow meeting larger demands and decreasing the relative cost of upstream activities. However they increase the protein load on chromatography steps resulting in an increase in the number of cycles or further investment in larger columns and hence the relative cost of downstream increases.[3,4] Although alternatives to traditional column chromatography platforms are emerging (e.g., non-chromatography operations, membrane adsorbers), industry practitioners are still reluctant to perform major process changes.[1–3] At the same time, it is important to determine how best to use existing installed production capacity for mAbs.[5,6] In this context, continuous improvement of existing processes, particularly the optimization of chromatography operations, is a valuable approach to address the current challenges. The development of computer-based decisional tools for the bioprocess sector is an emerging area[7–11] and frameworks have been developed to assess different solutions for the design and operation of chromatography steps. Joseph

Songsong Liu and Ana S. Simaria are joint first authors.

Correspondence concerning this article should be addressed to S. S. Farid at s.farid@ucl.ac.uk or L. G. Papageorgiou at l.papageorgiou@ucl.ac.uk.

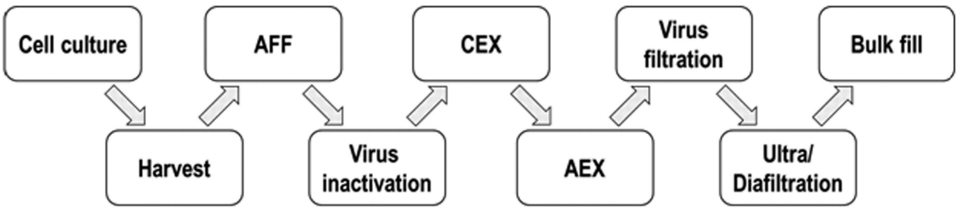

Figure 1. A typical mAb platform process.

et al.[12] present a simulation model to identify windows of operation for a chromatography step, using productivity and cost of goods (COG) as performance criteria. A model to find combinations of protein load and loading flow rate that meet yield and throughput constraints has been developed by Chhatre et al.[13] The discrete-event simulation framework proposed by Stonier et al.[14] allows the selection of optimal chromatography column sizes over a range of titers by brute force simulation. However, such an approach may not be feasible for very large decision spaces, and, particularly, when the variables have integer domain, as is the case in the problem addressed in the present article.

There are a large number of possible permutations and trade-offs related to running packed-bed chromatography operations such as opting for a smaller column run for several cycles so as to reduce resin costs vs. a large column run for fewer cycles so as to save time and labor costs. Decision makers usually have empirical approaches to come to a solution, mainly based on previous experience, and so may be missing good opportunities for improvement. The combinatorial optimization (CO) nature of the decision problem consists of selecting the most appropriate sizing strategy for the chromatography operation. In this article, the decisions are addressed using mixed-integer programming (MIP) techniques due to their widely recognized ability to handle CO problems.

Mixed-integer linear (MILP) and non-linear programming (MINLP) models have been developed to address capacity planning problems in the pharmaceutical[15,16] and biopharmaceutical[17,18] industries. At the process level, MIP models have focused on determining optimal purification sequences, using physicochemical data of protein mixtures and mathematical correlations of the separation techniques.[19–21] In some cases, the process synthesis optimization has also considered product loss by incorporating the decisions on the time of product collection and the start and finishing cut-points.[22,23] More recently, efficient MILP models were developed using the discretization[24] and piecewise linearization approximation[25] to overcome the computational expense of MINLP models. These models use the number of chromatography steps, purity, and yield as performance metrics, but do not account for overall process costs.

Optimization of chromatography equipment sizing strategies for a sequence of chromatography steps on the basis of a global criterion, such as cost of goods per gram (COG/g), requires the use of either MINLP approaches or heuristic search methods such as evolutionary algorithms to handle the complex model dependencies. Meta-heuristic methods have been developed that integrate evolutionary algorithms with detailed process economics models to determine the most cost-effective purification sequences and chromatography sizing strategies that meet purity constraints.[26,27] MINLP approaches have the advantage of providing exact solutions in the cases where commercial solvers or linearization techniques allow a feasible solution to be identified. However, an MINLP model for this problem domain does not exist in the literature. Hence, this article presents a novel mathematical programming model based on an MINLP formulation to determine the best chromatography equipment sizing strategies for the production of mAbs. The CO model addresses the challenge of optimizing the chromatography sizing strategy for a sequence of chromatography steps in a downstream purification train whilst considering several key decision variables for each step, including column bed height, column diameter, number of columns, and number of cycles. Furthermore, the model is used also to determine the optimal facility fit configuration for products with higher titers. A related problem has been previously addressed by Stonier et al.[28] using a stochastic simulation framework and multivariate analysis to identify root causes of facility mismatches.

The problem under study in this work—optimization of chromatography sizing strategies for facility design and facility fit—is formulated as an MINLP model, which can be solved to global optimality using commercially available global optimization solvers.

Problem Description

The problem addressed in this article is to determine the optimal equipment sizing strategies for a sequence of packed-bed chromatography columns used in the purification of mAbs. A typical mAb platform process is used in this study (as shown in Figure 1). In upstream processing (USP), mammalian cells expressing the mAb of interest are cultured in bioreactors. Then the broth moves to downstream processing (DSP), where the mAb is recovered, purified, and cleared from viruses using a variety of operations, such as different types of filtration, and a number of chromatography steps. The chromatography sequence includes three packed-bed chromatography steps, namely affinity (AFF) chromatography for product capture followed by cation-exchange (CEX) chromatography for intermediate purification, and anion-exchange (AEX) chromatography for polishing.

The problem addresses the challenges of dealing with multiple decisions, criteria, and constraints. This is further complicated by the sequential nature of decisions and their interdependencies, e.g. in a multi-step purification process the amount of resin required for a particular chromatography step depends on the equipment sizing strategy that was selected for the previous chromatography step. A schematic of the decision choices in this chromatography sizing problem is shown in Figure 2. The decisions at each chromatography step include the bed height, diameter, number of cycles, and number of columns to run in parallel at each step. The strategy selected has a direct impact on key metrics related to cost, time, and annual product output. This captures the trade-offs of using large columns with a single

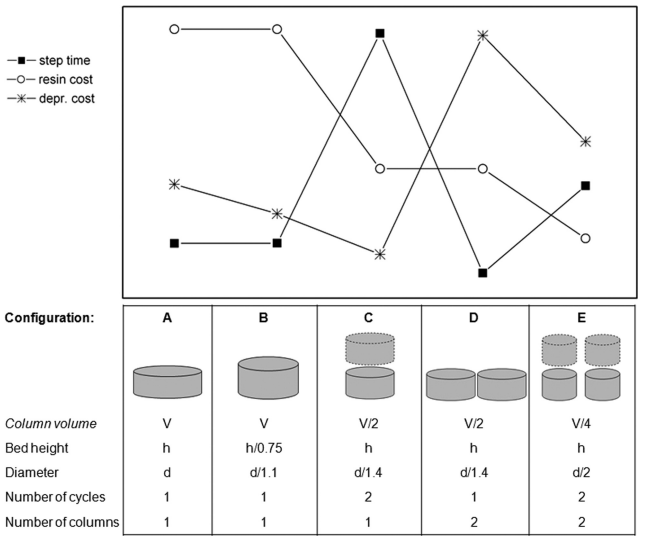

Figure 2. Comparison of alternative chromatography column sizing strategies in terms of the decision variables of the optimization problem (bed height, diameter, number of cycles, and number of columns) and the corresponding performance metrics of each configuration (step time, resin cost, and equipment depreciation cost). All the configurations allow processing the same amount of product (volume and mass). Column configurations with dotted outline indicate multiple cycles.

cycle vs. smaller columns with multiple cycles as illustrated in the schematic. Small changes in bed height were also accommodated to account for typical ranges seen in industrial applications and the use of multiple parallel columns per step was incorporated so as to determine whether this offered significant advantages that might outweigh current preferences to avoid parallel columns due to validation burdens.

In this problem, the USP trains work constantly so it is necessary to monitor the real DSP time such that the scheduling of batches between the USP and DSP trains occurs as originally planned. This model feature is very important as scenarios of multiple USP trains feeding a single DSP train are considered. It is assumed that multiple bioreactors operate in staggered mode and feed the DSP trains intermittently. Ideally, as soon as the cell culture is complete the product should enter the DSP train, hence an increase in the USP:DSP trains ratio corresponds not only to a decrease in the bioreactor(s) size, and hence on the batch size, but also to a decrease in the DSP window, i.e. the time available to perform the DSP operations. This might be a challenging scenario which requires an appropriate column sizing strategy in order to ensure that the DSP operations are performed within the DSP window.

The COG comprises both direct costs based on resource utilization (e.g., resin costs, buffer costs, and variable labor costs associated with DSP time) and indirect costs (e.g. facility-dependent overheads and capital costs). The total cost is then divided by the product output to compute the cost of goods per gram (COG/g). This is a standard approach[7] which allows the incorporation of multiple process features into a single metric. Particularly relevant to the current work is the relationship between annual product output and COG/g, as process configurations which result in lower product outputs are automatically penalized in terms of COG/g. The COG/g was used by the proposed mathematical programming model as the objective function to be minimized.

In this problem, the annual demand is an input of the model and it is used to calculate the bioreactor size and required number of batches, which is an upper bound of the number of completed batches. However, if a particular equipment sizing strategy leads to long processing times, it may not be possible to meet the required number of batches and hence the annual product output would be below the production target. This issue is indirectly addressed by the use of COG/g as objective function, which favors solutions with higher product output values. Thus, the annual product demand can be met, unless the DSP time exceeds the DSP window.

Overall, the problem addressed in this work is described as follows. The following parameters are inputs: the process sequence of a mAb product, the annual demand, the product titer, the ratio of USP to DSP trains, the key operating parameters of the chromatography operations (e.g., yield, linear velocity, buffer usage, resin dynamic binding capacity), the processing times of non-chromatography unit operations, cost data (e.g., reference equipment costs, labor rate, resin, buffer, and media prices), the column diameter and height candidates, and the maximum number of cycles and columns. Given these inputs, the goal is to determine the column sizing strategies (i.e., column diameter and height, the number of cycles, number of columns at each step), the number of completed batches, the total product output and the total annual cost so as to minimize COG/g.

Mathematical Formulation

An MINLP model was developed for the chromatography column sizing problem described in the previous section. Only the equations most relevant to the case study discussion are presented in the main text; the complete set of constraints is shown in Table A.1 (Appendix).

Calculation of input parameters

To initialize the model, the required number of batches to meet the annual demand was estimated, given the number of production bioreactors existing in the facility. This corresponds to the maximum number of batches that can be completed within the planning horizon:

$$\mathrm{Max}N^{\mathrm{batch}} = N^{\mathrm{bior}} \times \frac{T^{\mathrm{annu}}}{T^{\mathrm{bior}}} \tag{1}$$

where T^{annu} is the annual operating time, T^{bior} is the bioreaction time, and N^{bior} is the number of bioreactors. Then, the volume of a single bioreactor was estimated by the following expression:

$$V^{\mathrm{bior}} = \frac{\mathrm{Annu}D}{\mathrm{Max}N^{\mathrm{batch}} \cdot \sigma \cdot \alpha \cdot \mathrm{Titer} \cdot \prod_s \mathrm{Yd}_s} \tag{2}$$

where Annu$D$ is the annual demand, Yd_s is the yield of product at unit operation s, α is the bioreactor working volume ratio, "Titer" is the titer of the product and σ is the batch success rate. With the above two parameters defined and calculated, the proposed mathematical programming model is presented in the next section.

Product mass constraints

In each batch, the initial product mass entering the DSP train depends on the titer of the product and the working volume of production bioreactor (Eq. 3). The product mass after each unit operation s depends on its yield (Eq. 4).

$$M_0 = \text{Titer} \cdot \alpha \cdot V^{\text{bior}} \tag{3}$$

$$M_s = \text{Yd}_s \cdot M_{s-1}, \quad \forall s \tag{4}$$

The annual product output was determined using the product mass after the bulk fill operation (last operation in the process) per batch multiplied by the number of batches and the batch success rate.

$$\text{Annu}O = \sigma \cdot N^{\text{batch}} \cdot M_{\text{bf}} \tag{5}$$

N^{batch} was limited by the required number of batches to meet the demand, i.e., its upper bound given by Eq. 1.

$$N^{\text{batch}} \leq \text{Max}N^{\text{batch}} \tag{6}$$

Chromatography operation constraints

Resin Volume. The total column volume for chromatography step s was defined as the number of columns multiplied by the corresponding column volume.

$$\text{Tot}V_s^{\text{col}} = \sum_i V_{si}^{\text{col}} \cdot N_{si}^{\text{col}}, \quad \forall s \in \text{CS} \tag{7}$$

where V_{si}^{col} is the volume of the candidate column size i for chromatography step s, determined by specific diameter $\text{DM}_{si}^{\text{col}}$ and height H_{si}^{col}. Thus, if a column size i was selected, the corresponding diameter and bed height were both known. Here, it was assumed that only one column size could be selected for each step, for ease of validation, as defined by:

$$\sum_i X_{si}^{\text{col}} = 1, \quad \forall s \in \text{CS} \tag{8}$$

$$N_{si}^{\text{col}} \leq \text{Max}N_s^{\text{col}} \cdot X_{si}^{\text{col}}, \quad \forall s \in \text{CS}, i \tag{9}$$

where X_{si}^{col} is a binary variable to indicate whether column size i is selected for step s and $\text{Max}N_s^{\text{col}}$ represents its maximum number of columns.

The total amount of resin available must be sufficient to process all product mass entering this operation, so the number of cycles multiplied by the total column volume should be greater than the minimum required resin volume:

$$N_s^{\text{cyc}} \cdot \text{Tot}V_s^{\text{col}} \geq \text{Min}V_s^{\text{resin}}, \quad \forall s \in \text{CS} \tag{10}$$

The amount of resin required per batch, for a particular chromatography step, depends on the mass of product to be processed, the dynamic binding capacity of the resin used in that step, and the resin utilization factor:

$$\text{Min}V_s^{\text{resin}} = \frac{M_{s-1}}{\text{DBC}_s \cdot \mu}, \quad \forall s \in \text{CS} \tag{11}$$

Also, the number of cycles for each chromatography operation cannot exceed its upper bound:

$$N_s^{\text{cyc}} \leq \text{Max}N_s^{\text{cyc}}, \quad \forall s \in \text{CS} \tag{12}$$

Product and Buffer Volume. In both AFF and CEX operations, which operated in bind-and-elute mode (Eq. 13), the volume of the output product was equal to the eluate volume. In the flow-through AEX operation, it was assumed that the product volume did not change from the previous step (Eq. 14). The total buffer volume necessary to run a chromatography cycle was given by the buffer usage ratio multiplied by the total column volume (Eq. 15).

$$V_s^{\text{prod}} = \text{EluCV}_s \cdot N_s^{\text{cyc}} \cdot \text{Tot}V_s^{\text{col}}, \quad \forall s = \text{aff}, \quad \text{cex} \tag{13}$$

$$V_s^{\text{prod}} = V_{s-1}^{\text{prod}}, \quad \forall s = \text{aex} \tag{14}$$

$$V_s^{\text{buff}} = \text{BuffCV}_s \cdot N_s^{\text{cyc}} \cdot \text{Tot}V_s^{\text{col}}, \quad \forall s \in \text{CS} \tag{15}$$

Processing Time. In each chromatography step, the total processing time per batch was the summation of time for adding buffer and loading product.

$$T_s^{\text{dsp}} = T_s^{\text{prod}} + T_s^{\text{buff}}, \quad \forall s \in \text{CS} \tag{16}$$

When there were parallel columns, the product volume loaded to each column was the total product volume from the previous operation divided by the number of columns. The processing time for loading product was the product volume loaded to each column divided by the volumetric flow rate.

$$T_s^{\text{prod}} = \frac{V_{s-1}^{\text{prod}}}{\text{VFR}_s \cdot \sum_i N_{si}^{\text{col}}}, \quad \forall s \in \text{CS} \tag{17}$$

The volumetric flow rate (L/h) at a chromatographic operation was determined by the velocity (Vel_s) and column diameter as follows:

$$\text{VFR}_s = \left(\text{Vel}_s \cdot \pi \cdot \sum_i \left(\frac{\text{DM}_{si}^{\text{col}}}{2} \right)^2 \cdot X_{si}^{\text{col}} \right) \Big/ 1000, \quad \forall s \in \text{CS} \tag{18}$$

The processing time (h) for adding buffer is given by:

$$T_s^{\text{buff}} = \frac{\text{BuffCV}_s \cdot N_s^{\text{cyc}} \cdot \sum_i (V_{si}^{\text{col}} \cdot X_{si}^{\text{col}})}{\text{VFR}_s}, \quad \forall s \in \text{CS} \tag{19}$$

Batch time

As other non-chromatographic DSP operations are not the main concern of this problem, it was assumed that their operating times were constant. The total DSP time per batch was defined as the sum of the processing times of all DSP operations converted into days such that it reflects the shift pattern of DSP operators.

$$\text{Batch}T^{\text{dsp}} = \frac{\sum_s T_s^{\text{dsp}}}{N_{\text{shift}}^{\text{hour}} \cdot N^{\text{shift}}} \tag{20}$$

where $N_{\text{shift}}^{\text{hour}}$ indicates the number of hours per shift and N^{shift} indicates the number of shifts per day. If $\text{Batch}T^{\text{dsp}}$ is greater than the DSP window, $\text{Window}^{\text{dsp}} = \frac{T^{\text{bior}}}{N^{\text{bior}}}$, the required number of batches cannot be completed and the annual demand cannot be met.

The total annual DSP time was calculated by:

$$\text{Annu}T^{\text{dsp}} = N^{\text{batch}} \cdot \text{Batch}T^{\text{dsp}} \tag{21}$$

where $\text{Annu}T^{\text{dsp}}$ cannot exceed its upper bound:

Table 1. Characteristics of the Three Packed-Bed Chromatography Steps in the Case Study

Chromatography Step	Yield (Yd, %)	Resin Dynamic Binding Capacity (DBC, g/L)	Resin Price (Pc^{resin}, £/L)	Linear Velocity (Vel, cm/h)	Eluate Volume (EluCV, CV)	Buffer Volume (BuffCV, CV)
AFF	91	30	6,400	300	2.3	37
CEX	92	40	400	300	1.4	26
AEX	95	100	700	300	–	10

$$\text{Annu}T^{\text{dsp}} \leq T^{\text{annu}} - T^{\text{bior}} \tag{22}$$

Cost calculation

The total annual operating cost, Annu$C$, comprises both direct costs based on resource utilization (e.g., resin costs, buffer costs, and variable labor costs associated with DSP time) and indirect costs (e.g., facility-dependent overheads and capital costs). Due to space constraints, the description of the cost calculation constraints will be limited to the resin and equipment costs. The full calculation is presented in Table A.1 (Appendix).

Resin Cost. In this work, only the resin was considered to calculate the consumables cost, as the resin volume is a key decision in this problem. The cost for other consumables was ignored. Assuming that the resin would be re-used until it reaches its lifetime, the annual resin cost was calculated by:

$$C^{\text{resin}} = \sum_{s \in \text{CS}} \frac{A \cdot \text{Pc}_s^{\text{resin}} \cdot N^{\text{batch}} \cdot N_s^{\text{cyc}} \cdot \text{Tot}V_s^{\text{col}}}{L} \tag{23}$$

where $\text{Pc}_s^{\text{resin}}$ is the resin price, A is the over-packing factor for resin, and L is the resin lifetime (in terms of number of cycles).

Equipment Cost. Given the nature of the optimization problem addressed as well as the case study scenarios analyzed in this article, the two types of equipment considered for the calculation of indirect costs were the production bioreactors and chromatography columns. For different sizes of chromatography columns and bioreactors, the costs were calculated by using the values of reference equipment sizes and costs to scale-up the equipment cost:

$$C_{si}^{\text{col}} = \text{Ref}C^{\text{col}} \cdot \left(\frac{\text{DM}_{si}^{\text{col}}}{\text{RefDM}^{\text{col}}} \right)^{\text{SUF}^{\text{col}}} \tag{24}$$

$$C^{\text{bior}} = \text{Ref}C^{\text{bior}} \cdot \left(\frac{V^{\text{bior}}}{\text{Ref}V^{\text{bior}}} \right)^{\text{SUF}^{\text{bior}}}, \tag{25}$$

where $\text{Ref}C^{\text{col}}$ is the cost of a single chromatography column with a diameter of $\text{RefDM}^{\text{col}}$, and $\text{Ref}C^{\text{bior}}$ is the cost of a single bioreactor with a volume of $\text{Ref}V^{\text{bior}}$. Both reference costs are used to scale up the costs of chromatography columns and bioreactors with different sizes, using SUF^{col} and SUF^{bior} as the scale-up factors for columns and bioreactors, respectively. The equipment cost was then used to calculate the capital investment value.

Objective function

In the work, the objective was to minimize COG/g, which equals to the annual total cost divided by the annual product output. Thus, COG/g can be expressed as:

Table 2. Candidate Values of the Column Sizing Decision Variables in the Case Study

Decision Variable	Candidate Value
Bed height (H^{col}, cm)	15, 16, 17, 18, 19, 20, 21, 22, 23, 24, 25
Diameter (DM^{col}, cm)	50, 60, 70, 80, 90, 100, 120, 160, 180, 200
Number of cycles (N^{cyc})	1, 2, 3, 4, 5, 6, 7, 8, 9, 10
Number of columns (N^{col})	1, 2, 3, 4

$$z = \frac{\text{Annu}C}{\text{Annu}O} \tag{26}$$

Overall, the problem was formulated as an MINLP model with Eqs. (3–25) as key constraints and with Eq. 26 as the objective function. A number of constraints in the proposed model are nonlinear, which involve bilinear (e.g., Eq. 5) or trilinear terms (e.g., Eq. 23). Also, the objective function is a fraction of two variables. The nature of the nonlinearity in the model leads to high computational complexity to find the global optimum. The complete set of the model constraints is presented in Table A.1 (Appendix).

Case Study Setup

The MINLP model was applied to an industrially relevant case study, based on a biopharmaceutical company using a platform process for mAb purification to manufacture a single product with a demand of 500 kg/year and a titer of 3 g/L. The key parameters of the considered three packed-bed chromatography steps are shown in Table 1 and the candidate values of the chromatography equipment sizing decision variables are shown in Table 2. As there are 11 possible bed heights and 10 possible diameters, a single column has 110 possible volumes. The number of cycles can be up to 10, while at most 4 columns are allowed to be used in parallel. The complete set of data used in the MINLP model for the case study is shown in Table A.1 (Appendix), alongside the corresponding model constraints. The parameter values used in this case study were similar to the ones presented in Simaria et al.[26]

The goal was to design a new facility that was able to (a) manufacture the product in a cost-effective manner and (b) cope with predicted future higher titers. To address the first goal, the MINLP model described in Section "Mathematical Formulation" was run using the current product titer (3 g/L) and this model was named $\text{MINLP}_{\text{Design}}$. In order to address the second goal, the original model was modified to account for facility fit constraints, resulting in a second model $\text{MINLP}_{\text{Facility-fit}}$. In this model, the size of the production bioreactor(s) was fixed to represent an existing facility (instead of calculated by Eq. 2) and the maximum column diameter was dictated by the existing facility and therefore the degrees of freedom of the model to achieve the minimum COG/g were the column bed height and number of cycles. Future products in the pipeline were expected to have titers up to 15 g/L and so the values 6, 9, 12, and 15g/

Table 3. Characteristics of the MINLP Models

Model	$MINLP_{Design}$	$MINLP_{Facility\text{-}fit}$	
Version		A	B
Goal	Design a new facility for current titer.	Fit process with higher titers to existing facility.	Increase DSP capacity
Description	As described in section 3.	Bioreactor and column sizes given by $MINLP_{Design}$; bed height and number of cycles can change.	Bioreactor and column sizes given by $MINLP_{Design}$; bed height and number of cycles can change and additional columns can be installed.
Model variables			
Bioreactor size	Calculated	Given by $MINLP_{Design}$	
Column diameter	Decision variable	Given by $MINLP_{Design}$	
Number of columns	Decision variable	Given by $MINLP_{Design}$	Decision variable
Handling of mass loss	No mass loss occurs	New continuous variable: $MLoss_s$ Modified constraints to replace Eqs. 4 and 11:	

$$M_s = \mathrm{Yd}_s \cdot (M_{s-1} - \mathrm{MLoss}_s|_{s\in \mathrm{CP}}),\ \forall s \tag{4a}$$

$$\mathrm{Min}V_s^{\mathrm{resin}} = \frac{M_{s-1} - \mathrm{MLoss}_s}{\mathrm{DBC}_s \cdot \mu},\ \forall s \in \mathrm{CP} \tag{11a}$$

Modified objective function to replace Equation 26:

$$z = \frac{\mathrm{Annu}C + U \cdot \sum_{s\in \mathrm{CP}} \mathrm{MLoss}_s}{\mathrm{Annu}O} \tag{26a}$$

where U is a penalty weight for mass loss

L were considered in the study. Given the fixed bioreactor volume, higher titers meant higher product masses entering into each chromatographic purification operation, increasing the required resin volume, as given by Eq. 11. However, as the number of columns and column diameters were fixed, and the maximum bed height and number of cycles were limited, it was important to account for product being discarded when the required resin volumes could not be met.

To model the above situation, a new continuous variable, $MLoss_s$ for the protein mass loss at chromatography step s was introduced in the $MINLP_{Facility\text{-}fit}$ model. The product mass entering chromatography operation s should be the product mass after the previous operation, M_{s-1}, minus the product mass loss at this chromatography operation, $MLoss_s$, due to the lack of resin capacity at step s. The product mass after operation s, M_s, and the amount of resin required per batch, $MinV_s^{resin}$, was formulated considering the mass loss, using two new constraints to replace Eqs. 4 and 11, as shown in Table 3. Also, an alternative objective to penalize the product loss was introduced (Table 3), in which U was developed as a penalty weight for mass loss. Computational tests on the case study showed that when $U <$ 100, the optimal solution could be obtained. In this case study U was set to 10 in all scenarios.

In order to assess different strategies of increasing the facility's capacity, two versions of the $MINLP_{Facility\text{-}fit}$ model were developed as presented in Table 3. In version A, the number of columns running in parallel at each chromatography step, N_{si}^{col}, was fixed to the values obtained from the $MINLP_{Design}$ model, while version B allowed the installation of additional columns by letting the decision variable N_{si}^{col} change. In the latter situation it was assumed that the parallel columns were equally sized given industry preferences for ease of validation and operation.

Three different ratios of USP to DSP trains were considered (1:1, 2:1, and 4:1) so as to evaluate which configuration would be most suitable in terms of cost-effectiveness and robustness to cope with higher titers. The different USP:DSP configurations will have an impact of the size of the bioreactor(s) as well as on the DSP window, i.e. the time available to perform the DSP operations, as it is assumed that multiple bioreactors are operated in a staggered mode, feeding a single DSP train intermittently.

Results and Discussion

The proposed optimization models were implemented in GAMS 23.9[29] using the global MINLP solver BARON on a 64-bit Windows 7 based machine with 3.20 GHz six-core Intel Xeon processor W3670 and 12.0 GB RAM. The $MINLP_{Design}$ model, with 403 constraints, 73 continuous variables, and 664 discrete variables, took less than 1,200 sec to find the optimal solution for each scenario. The number of variables in the $MINLP_{Facility\text{-}fit}$ model depended on the solution of the $MINLP_{Design}$ model, and its CPU time was tens of seconds for all scenarios investigated in the case study.

New facility design for current titers ($MINLP_{Design}$)

Figure 3 summarizes the characteristics of the optimal solutions provided by $MINLP_{Design}$ model for the different USP:DSP ratios analyzed in the case study, in terms of the volume of the columns and number of cycles of each chromatography step (Figure 3a), cost metrics (Figure 3b), and kg product output metrics (Figure 3c). In all the scenarios examined, single columns were selected for each purification step. With the increasing number of USP trains, the optimal solutions were characterized by using similar column volumes but running for fewer cycles to shorten the DSP time such that it fitted within tighter DSP windows. The DSP windows were 15, 7.5, and 3.8 days for 1USP:1DSP, 2USP:1DSP, and 4USP:1DSP configurations, respectively.

The value of the objective function COG/g was lowest for the scenario of 1USP:1DSP, where a single bioreactor was used, and it increased with the number of USP trains as illustrated in Figure 3b. This can be attributed to the higher investment cost and hence indirect costs (e.g., depreciation) per gram associated with installing multiple smaller bioreactors vs. a single large bioreactor due to economies of scale as well as the increased labor costs associated with running multiple bioreactors. Hence a trade-off exists between the

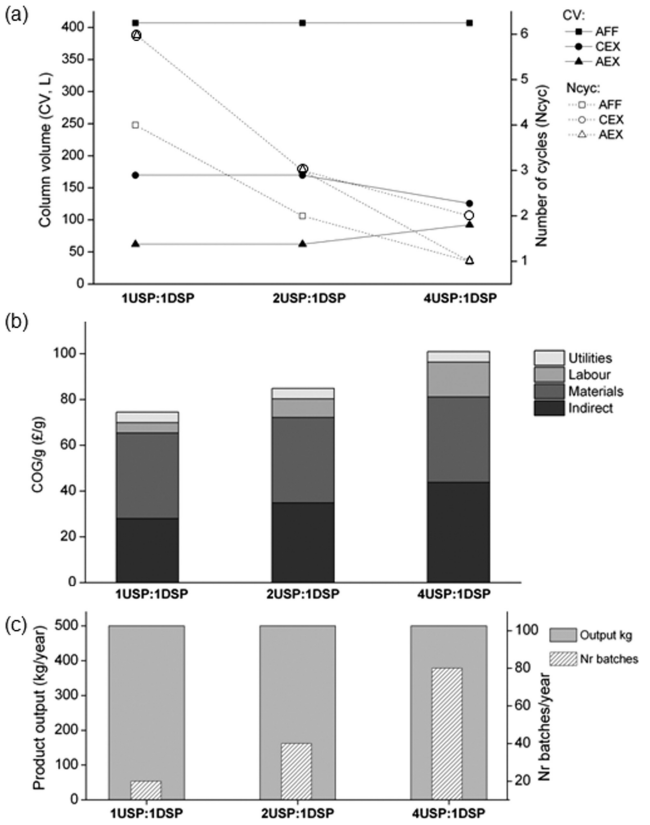

Figure 3. Comparison of the characteristics of the optimal solutions provided by the MINLP model for the different USP:DSP scenarios in terms of (a) column volume and number of cycles, (b) COG/g with corresponding breakdown, (c) product output and number of batches manufactured per year. Results are shown for the scenario where a new facility was designed for manufacturing a product with titer of 3 g/L and demand of 500 kg/year.

lower COG/g with a single bioreactor set-up vs. the lower risk (and hence mass loss) consequences, greater equipment utilization, and potentially greater agility with smaller staggered bioreactor set-ups. Besides the value of COG/g, other criteria were used to assess the different USP:DSP ratios, and provide a more complete decision-support framework for biopharmaceutical facility design. The next section presents the results and discussion regarding the ability of a facility to cope with higher titer values.

Impact of higher titers on facility design ($MINLP_{Facility\text{-}fit}$)

In order to evaluate the impact of higher titers on the facility design, the results obtained by the model $MINLP_{Design}$ (namely, bioreactor volumes and column diameters) were used as inputs to the $MINLP_{Facility\text{-}fit}$ model (versions A and B). The set of optimal solutions found by the MINLP models for the different case study scenarios is presented in Table 4 and visually displayed in Figure 5. The values in bold in Table 4 represent scenarios where mass loss could only be avoided by the installation of parallel chromatography columns. For these situations, at least one of the chromatography steps reached the maximum limit of all column sizing variables allowed to change in the $MINLP_{Facility\text{-}fit\_A}$ (bed height and number of cycles) and any excess mass entering the column was lost. The model $MINLP_{Facility\text{-}fit\_B}$ was solved in order to obtain a solution without mass loss. This was observed for the 1USP:1DSP scenario at titers equal to or greater than 6g/L and for the 2USP:1DSP configuration for titers 12 and 15 g/L.

Figure 4 shows a comparison between the optimal solutions of $MINLP_{Facility\text{-}fit\_A}$ (Figure 4a) and $MINLP_{Facility\text{-}fit\_B}$ (Figure 4b) models in terms of COG/g and product output, for different titer values in the 1USP:1DSP scenario. As titer increased more product mass was processed per batch hence increasing the total annual product output. However, due to

Table 4. Characteristics of the Optimal Solutions Found by the MINLP Models for the Different Case-Study Scenarios

MINLP Model	Design			Facility-Fit A		Facility-Fit B		Facility-Fit A		Facility-Fit B	Facility-Fit A	
USP:DSP	1:1	2:1	4:1	1:1		1:1		2:1		2:1	4:1	
Titer (g/L)	3	3	3	6	15	6	15	6	15	15	6	15
DSP window (days)	15	7.5	3.8	15		15		7.5		7.5	3.8	
Maximum number of batches/year	20	40	80	20		20		40		40	80	
Bioreactor volume (L)	21,668	10,834	5,417	21,668		21,668		10,834		10,834	5,417	
AFF bed height (cm)	16	16	16	25	25	16	16	16	25	20	16	20
AFF number of cycles	4	2	1	5	5	8	10	4	5	4	2	4
AFF diameter (cm)	180	180	180	180	180	180	180	180	180	180	180	180
AFF number of columns	1	1	1	1	1	1	**2**	1	1	**2**	1	1
CEX bed height (cm)	15	15	16	17	17	18	25	18	17	16	16	16
CEX number of cycles	6	3	2	10	10	10	9	5	10	7	4	10
CEX diameter (cm)	120	120	100	120	120	120	120	120	120	120	100	100
CEX number of columns	1	1	1	1	1	1	**2**	1	1	**2**	1	1
AEX bed height (cm)	22	22	24	25	25	22	22	22	25	21	24	24
AEX number of cycles	6	3	1	10	10	6	10	6	10	8	2	5
AEX diameter (cm)	60	60	70	60	60	60	60	60	60	60	70	70
AEX number of columns	1	1	1	1	1	**2**	**3**	1	1	**2**	1	1
Mass loss (kg/year)	0	0	0	**70**	**2849**	0	0	0	**907**	0	0	0
DSP time (days)	5.9	4.1	3.4	8.7	8.7	8.2	9.8	5.7	8.6	6.4	4.3	6.9
Number of batches/year	20	40	80	20	20	20	20	40	34	40	69	42
COG (£/g)	74.5	84.8	100.9	44.1	44.1	42.9	23.9	47.9	31.9	25.9	59.6	37.1
Product output (kg/year)	500	500	500	962	962	1000	2500	1000	1636	2500	863	1313

Note: The values in bold represent scenarios where mass loss could only be avoided by the installation of parallel chromatography columns. The underlined values represent input data of the corresponding model

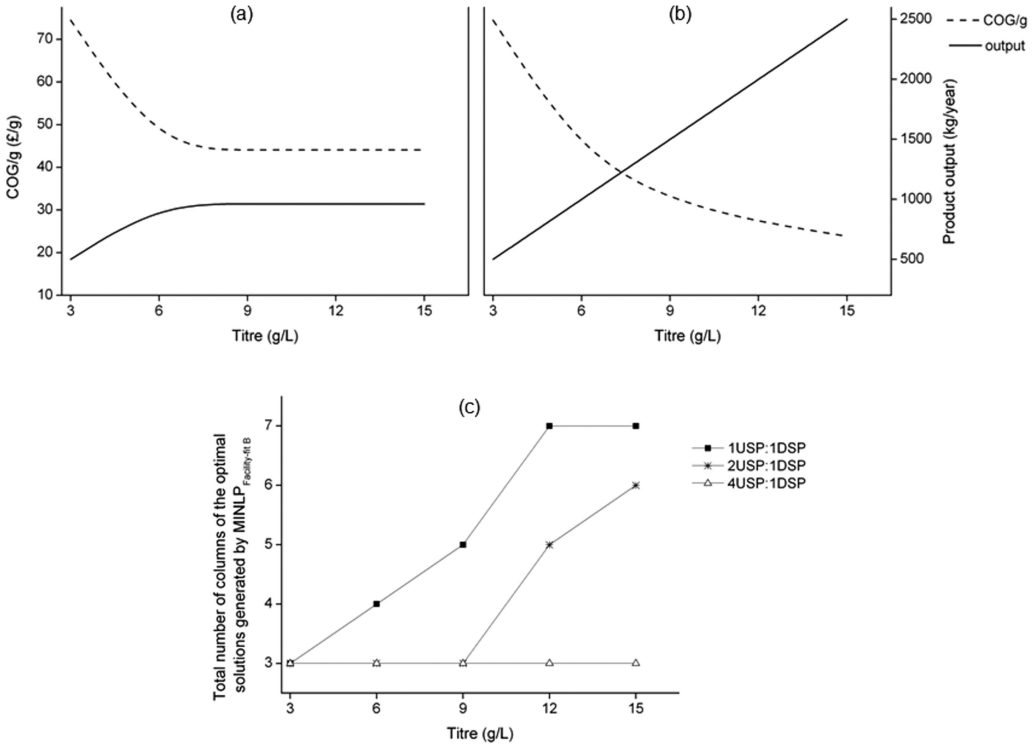

Figure 4. COG/g and annual product output of the optimal solutions of the models (a) $MINLP_{Facility\text{-}fit\_A}$ and (b) $MINLP_{Facility\text{-}fit\_B}$ for the 1USP:1DSP scenario across different titer values. (c) Total number of columns of the optimal solutions obtained by the $MINLP_{Facility\text{-}fit\_B}$ model for different USP:DSP ratios. The model $MINLP_{Facility\text{-}fit\_A}$ allows the increase of bed height and number of cycles of a chromatography step to cope with higher titers, while the model $MINLP_{Facility\text{-}fit\_B}$ also allows increasing the number of columns to run in parallel. The full details of these models are presented in Table 3.

the mass loss that occurred in the optimal solutions of the model $MINLP_{Facility\text{-}fit\_A}$, a flattening of the output and COG/g curves was observed in Figure 4a. In this situation, the increase in titer did not translate into a reduction in COG/g. The penalization in the objective function given by Eq. 26a in Table 3 minimizes the amount of mass loss but it does not avoid its occurrence. The absence of mass loss was achieved by the optimal solutions of the $MINLP_{Facility\text{-}fit\_B}$ model and this was obtained by increasing the number of columns running in parallel in the bottleneck steps, as shown in Table 4 and Figure 5. This resulted in an increase of product output and consequent reduction in COG/g, depicted in Figure 4b. For the scenario 2USP:1DSP, mass loss occurred for titers of 12 g/L and above. For the scenario of 4USP:1DSP, there was no mass loss even for the highest titer values, and so both $MINLP_{Facility\text{-}fit\_A}$ and $MINLP_{Facility\text{-}fit\_B}$ models produced the same optimal solutions This was due to the low number of cycles initially determined by the $MINLP_{Design}$ model which allowed the increase to a higher value without reaching the maximum limit. Note that although there was no mass loss at higher titers in the 4USP:1DSP scenario, the annual product output was not fully achieved. The increase in the number of cycles required to meet resin constraints led to DSP times which exceeded the DSP window, reducing the total number of batches that could be produced in a year. This is shown in the last two columns of Table 4.

The results of the case study were used to predict the critical titer levels where multiple parallel columns were needed to remove bottlenecks. In a 2USP:1DSP configuration (2 × 10,834 L bioreactors) parallel columns were required for titers of 12 g/L and above (harvest mass = 130 kg) while for 1USP:1DSP configurations this occurred at titer values of 6 g/L (1 × 21,668 L bioreactor, harvest mass = 130 kg). For the 4USP:1DSP facility configuration, the titer would need to be over 20 g/L for multiple columns to be required per step, given the column sizes installed. This value exceeds expected titer values for routine performance in the near future. Thus, it can be seen that although the configurations with multiple smaller bioreactors are more expensive to run they will be more robust to titer increases that could be expected in the future.

Facility design selection

The case study considered different independent USP:DSP scenarios that were used as model input parameters. In this section, that approach was taken further and the results of the case study were used to generate a decision-making framework for selecting the best USP:DSP configuration.

Assuming that no mass loss is desired, there are three different facility designs generated by the MINLP models described in this work, one for each USP:DSP scenario considered in the study, as shown in Figure 5. Each design is adapted to the product titer (e.g., increasing the number of cycles or using additional columns) but the facility is designed with that flexibility inbuilt. For example, multiple columns in parallel are installed and only used when necessary, as opposed to retrofitting the facility in the future. In light of these assumptions, an analysis of the trade-offs between the different alternatives is displayed in Figure 6. The line represents the Pareto front with the three solutions that establish a compromise between the average COG/g (calculated over the titer range) and the number of columns in the facility necessary to cope with the highest titer value considered in the case study. Larger columns with fewer batches per year offer economies of scale (e.g.,

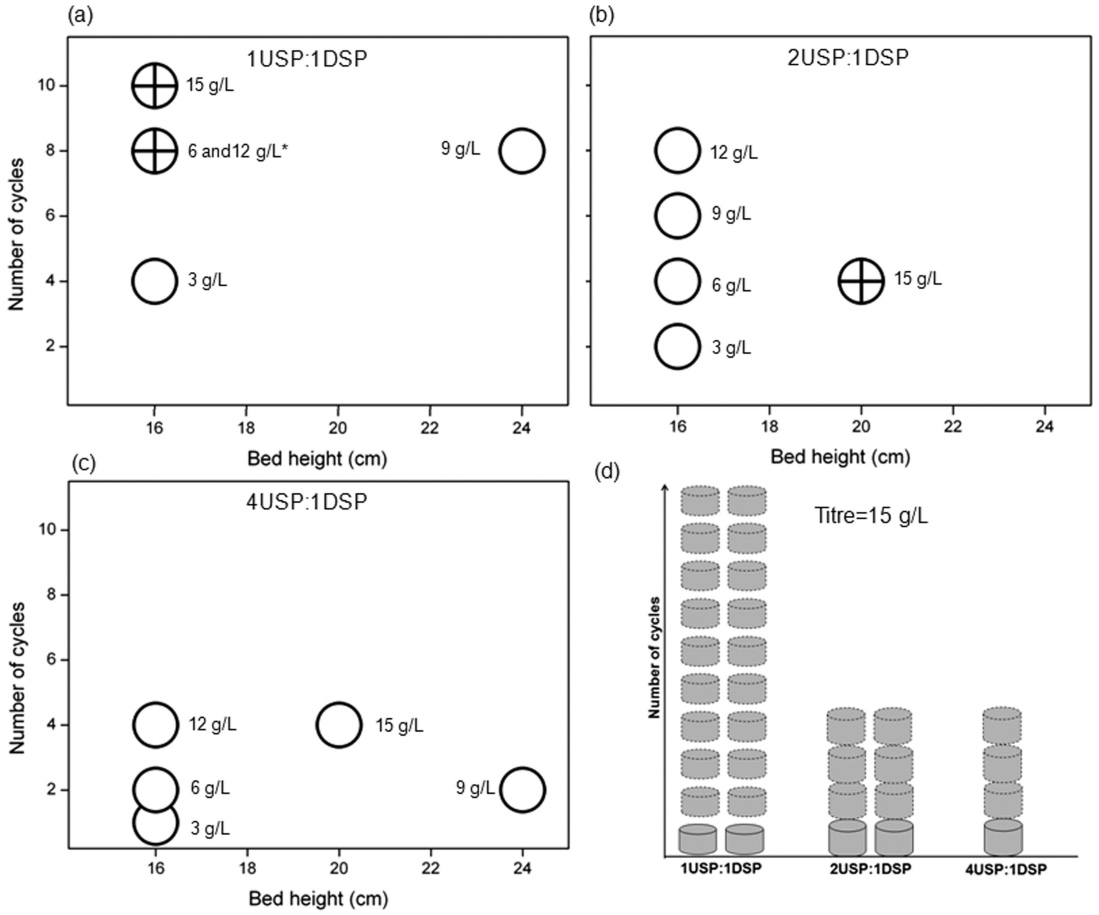

Figure 5. Characteristics of the optimal column sizing strategies (bed height (*x*-axis), number of cycles (*y*-axis) and number of columns (hollow bubbles represent a single column and crossed bubbles represent a solution where two columns are used in parallel) obtained by the MINLP models for the AFF step, for different titers and USP:DSP train ratios of (a) 1:1, (b) 2:1, and (c) 4:1. *For 6 g/L a single column is used and for 12 g/L two columns are used. The column diameter of the optimal solutions is 180 cm for all scenarios. A schematic of the optimal configurations obtained for titer 15 g/L is shown in (d).

1USP:1DSP) but high titers will increase the load on the DSP stage and additional columns will be required to avoid mass loss. If companies are not keen to operate multiple parallel columns for a particular step due to validation concerns, then a facility design with smaller batches (e.g., 4USP:1DSP) could be selected leading to higher COG/g values.

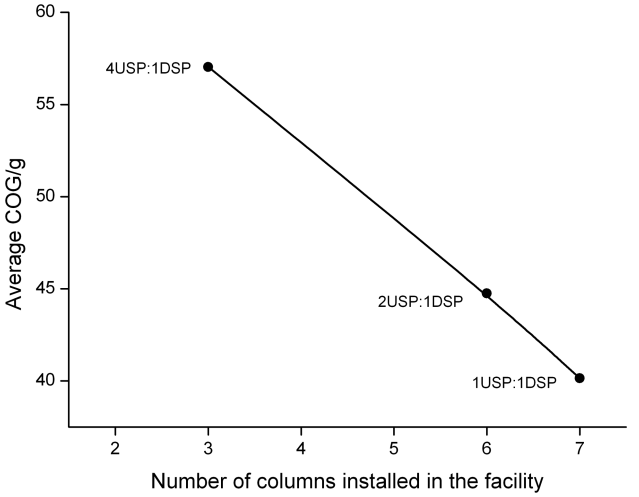

Figure 6. Comparison between the facility designs that result in no mass loss obtained by the MINLP models in the case study. Average COG/g = average COG/g of the MINLP optimal solutions of a particular USP:DSP ratio across the titer range. The line represents the Pareto front, i.e. solutions that present a trade-off between the average COG/g and the number of columns to be installed in the facility.

Conclusion

In this work, an MINLP modeling framework was proposed and applied to an industrially relevant case study to optimize the design of a facility by determining the most cost-effective chromatography equipment sizing strategies for the production of mAbs. Furthermore, the framework was used to evaluate the ability of the facility to cope with higher product titers, and to explore the trade-offs between alternative facility designs. The case study insights demonstrate that the proposed modeling approach can act as a valuable decision-support tool for the design of cost-effective facility configurations and to aid facility fit decisions. Future work will focus on extending the models to address chromatography sequencing decisions, incorporate uncertainty, and consider multi-objective optimization.

Acknowledgments

Funding from the UK Engineering & Physical Sciences Research Council (EPSRC) for the EPSRC Centre for Innovative Manufacturing in Emergent Macromolecular Therapies hosted by University College London is gratefully

acknowledged. Financial support from the consortium of industrial and governmental users is also acknowledged.

Notation

The mathematical formulation of the MINLP model is presented with the following notation:

Indices

aex = anion-exchange chromatography step
aff = affinity chromatography step
bf = bulk fill step
cex = cation-exchange chromatography step
i = column size
s = downstream step

Sets

CS = set of chromatography steps, $=\{\text{aff}, \text{cex}, \text{aex}\}$

Parameters

A = overpacking factor for resin
Annu$D$ = annual product demand, g
BuffCV_s = total buffer usage of resin at chromatography step s, column volume (CV)
DBC_s = dynamic binding capacity of resin at chromatography step s, g/L
$\text{DM}_{si}^{\text{col}}$ = diameter of column size i at step s, cm
EluCV_s = eluate volume of resin at chromatography step s, CV
H_{si}^{col} = bed height of column size i at step s, cm
L = resin life time, number of cycles
$\text{Max}N^{\text{batch}}$ = maximum number of batches per year
$\text{Max}N_s^{\text{col}}$ = maximum number of columns at chromatography step s
$\text{Max}N_s^{\text{cyc}}$ = maximum number of cycles at chromatography step s
N^{bior} = number of production bioreactors
$N_{\text{shift}}^{\text{hour}}$ = number of hours per shift
N^{shift} = number of shifts per day
$\text{Pc}_s^{\text{resin}}$ = resin price at chromatography step s, £/L
$\text{Ref}C^{\text{bior}}$ = reference cost of bioreactor, £
$\text{Ref}C^{\text{col}}$ = reference cost of column, £
$\text{RefDM}^{\text{col}}$ = reference diameter of column, cm
$\text{Ref}V^{\text{bior}}$ = reference volume of bioreactor, L
SUF^{bior} = scale-up factor of bioreactor
SUF^{col} = scale-up factor of column
T^{annu} = annual operating time, days
T^{bior} = bioreaction time, days
Titer = product titer, g/L
V_{si}^{col} = volume of column size i at step s, L
Vel_s = linear velocity of resin at chromatography step s, cm/h
$\text{Window}^{\text{dsp}}$ = DSP window, days
Yd_s = product yield of operation s
α = bioreactor working volume ratio
μ = chromatography resin utilization factor
σ = batch success rate

Continuous Variables

Annu$C$ = annual cost, £
Annu$O$ = annual product output, g
AnnuT^{dsp} = annual downstream processing time, days
BatchT^{dsp} = processing time of each batch, days
C^{bior} = bioreactor cost, £
C_{si}^{col} = cost of column of size i at chromatography step s, £
C^{resin} = resin cost, £
$\text{Min}V_s^{\text{resin}}$ = minimum resin volume required at chromatography step s, L
M_0 = initial product mass entering DSP, g
M_s = product mass after operation s, g
T_s^{dsp} = processing time of operation s, h
T_s^{prod} = processing time for loading product at chromatography step s, h
T_s^{buff} = processing time for adding buffer at chromatography step s, h
$\text{Tot}V_s^{\text{col}}$ = total column volume at chromatography step s, L
VFR_s = volumetric flow rate at chromatographic step s, L/h
V_s^{buff} = buffer volume used in chromatography step s, L
V_s^{prod} = product volume after operation s, L
z = optimization objective, cost of goods per gram, £/g

Binary Variables

X_{si}^{col} = 1 if column size i is selected for chromatography operation s; 0 otherwise

Integer Variables

N^{batch} = number of completed batches
N_{si}^{col} = number of columns of size i at chromatography step s
N_s^{cyc} = number of cycles at chromatography step s

Literature Cited

1. Low D, O'Leary R, Pujar NS. Future of antibody purification. *J Chromatogr B Analyt Technol Biomed Life Sci*. 2007;848:48–63.
2. Langer E. Downstream factors that will continue to constrain manufacturing through 2013. *BioProcessing J*. 2009;8:22–26.
3. Pujar NS, Low D, O'Leary R. Antibody purification: drivers of change. In: Gottschalk U, editor. Process Scale Purification of Antibodies. New Jersey: Wiley; 2009:407–426.
4. Farid SS. Process economic drivers in industrial monoclonal antibody manufacture. In: Gottschalk U, editor. Process Scale Purification of Antibodies. New Jersey: Wiley; 2009:239–261.
5. Kelley B. Very large scale monoclonal antibody purification: the case for conventional unit operations. *Biotechnol Prog*. 2007;23:995–1008.
6. Kelley B. Industrialization of mAb production technology: the bioprocessing industry at a crossroads. *mAbs*. 2009;1:443–452.
7. Farid SS, Washbrook J, Titchener-Hooker NJ. Decision-support tool for assessing biomanufacturing strategies under uncertainty: stainless steel versus disposable equipment for clinical trial material preparation. *Biotechnol Prog*. 2005;21:486–497.
8. Farid SS, Washbrook J, Titchener-Hooker NJ. Modelling biopharmaceutical manufacture: design and implementation of SimBiopharma. *Comput Chem Eng*. 2007;31:1141–1158.
9. Lim AC, Zhou Y, Washbrook J, Sinclair A, Fish B, Francis R, Titchener-Hooker NJ, Farid SS. Application of a decision-support tool to assess pooling strategies in perfusion culture processes under uncertainty. *Biotechnol Prog*. 2005;21:1231–1242.
10. Lim AC, Washbrook J, Titchener-Hooker NJ, Farid SS. A computer-aided approach to compare the production economics of fed-batch and perfusion culture under uncertainty. *Biotechnol Bioeng*. 2006;93:687–697.
11. Chhatre S, Jones C, Francis R, O'Donovan K, Titchener-Hooker NJ, Newcombe A Keshavarz-Moore E. The integrated

simulation and assessment of the impacts of process change in biotherapeutic antibody production. *Biotechnol Prog*. 2006;23: 1612–1620.
12. Joseph JR, Sinclair A, Tichener-Hooker NJ, Zhou Y. A framework for assessing the solutions in chromatographic process design and operation for large-scale manufacture. *J Chem Technol Biotechnol*. 2006;81:1009–1020.
13. Chhatre S, Thillaivinayagalingam P, Francis R, Titchener-Hooker NJ, Newcombe A Keshavarz-Moore E. Decision-support software for the industrial-scale chromatographic purification of antibodies. *Biotechnol Prog*. 2007;23:888–894.
14. Stonier A, Simaria AS, Smith M, Farid SS. Decisional tool to assess current and future process robustness in an antibody purification facility. *Biotechnol Prog*. 2012;28:1019–1028.
15. Papageorgiou LG, Rotstein GE, Shah N. Strategic supply chain optimization for the pharmaceutical industries. *Ind Eng Chem Res*. 2001;40:275–286.
16. Levis AA, Papageorgiou LG. A hierarchical solution approach for multi-site capacity planning under uncertainty in the pharmaceutical industry. *Comput Chem Eng*. 2004;28: 707–725.
17. Lakhdar K, Zhou Y, Savery J, Titchener-Hooker N J, Papageorgiou LG. Medium term planning of biopharmaceutical manufacture using mathematical programming. *Biotechnol Prog*. 2005;21:1478–1489.
18. Lakhdar K, Savery J, Papageorgiou LG, Farid SS. Multiobjective long-term planning of biopharmaceutical manufacturing facilities. *Biotechnol Prog*. 2007;23:1383–1393.
19. Vasquez-Alvarez E, Pinto JM. Efficient MILP formulations for the optimal synthesis of chromatographic protein purification processes. *J Biotechnol*. 2004;110:295–311.
20. Simeonidis E, Pinto JM, Lienqueo ME, Tsoka S, Papageorgiou LG. MINLP models for the synthesis of optimal peptide tags and downstream protein processing. *Biotechnol Prog*. 2005;21: 875–884.
21. Natali JM, Pinto JM, Papageorgiou LG. Efficient MILP formulations for the simultaneous optimal peptide tag design and downstream processing synthesis. *AIChE J*. 2009;55:2303–2317.
22. Vasquez-Alvarez E, Pinto JM. A mixed integer linear programing model for the optimal synthesis of protein purification processes with product loss. *Chem Biochem Eng Q*. 2003;17: 77–84.
23. Polykarpou EM, Dalby PA, Papageorgiou LG. Optimal synthesis of chromatographic trains for downstream protein processing. *Biotechnol Prog*. 2011;27:1653–1660.
24. Polykarpou EM, Dalby PA, Papageorgiou LG. A novel efficient optimisation system for purification process synthesis. *Biochem Eng J*. 2012;67:186–193.
25. Polykarpou EM, Dalby PA, Papageorgiou LG. An MILP formulation for the synthesis of protein purification processes. *Chem Eng Res Des*. 2012;90:1262–1270.
26. Simaria AS, Turner R, Farid SS. A multi-level metaheuristic algorithm to optimise antibody purification processes at the bioprocess business interface. *Biochem Eng J*. 2012;69:144–154.
27. Allmendinger R, Simaria AS, Farid SS. Efficient discovery of chromatography equipment sizing strategies for antibody purification processes using evolutionary computing. *Parallel Problem Solving Nature PPSN XII*. 2012;7492:468–477.
28. Stonier A, Pain D, Westlake A, Hutchinson N, Thornhill N, Farid SS. Integration of stochastic simulation with multivariate analysis: short-term facility fit prediction. *Biotechnol Prog*. 2013;29:368–377.
29. Brooke A, Kendrick D, Meeraus A, Raman R. GAMS—A User's Guide. Washington, D.C.: GAMS Development Corporation; 2012.

Appendix

Notation (additional to Section "Mathematical Formulation")

Indices

h	harvest step
ufdf	ultrafiltration/diafiltration step
vf	virus filtration step
vi	virus inactivation step

Parameters

a,b,c	utilities cost coefficients
DFV_s	diafiltration volume
FConc	final concentration of product
$\mathrm{Flu}V_s$	flush volume
GEF	general equipment factor
GU	general utility unit cost
Lang$F$	Lang factor
N^{operD}	number of operators for DSP
N^{operU}	number of operators per bioreactor in USP
$\mathrm{Neu}V_s$	neutralization volume
ny	project length, year
$\mathrm{Pc}^{\mathrm{buff}}$	buffer price
$\mathrm{Pc}^{\mathrm{media}}$	cell culture media price
r	interest rate
W	labor rate
θ	media overfill allowance
λ^{otheq}	other equipment cost factor
$\lambda^{\mathrm{othindirect}}$	other indirect costs factor
$\lambda^{\mathrm{othlabor}}$	other labor cost factor
λ^{misc}	miscellaneous material cost factor

Continuous variables

$\mathrm{Annu}V^{\mathrm{buff}}$	annual buffer volume
C^{buff}	buffer cost
C^{capital}	capital cost
$C^{\mathrm{directlab}}$	direct labor cost
C^{labor}	labor cost
C^{media}	media cost
$C^{\mathrm{othindirect}}$	other indirect costs
$C^{\mathrm{utilities}}$	utilities cost
FCI	fixed capital investment
V_0^{prod}	initial product volume entering DSP

Table A.1. Complete Set of Constraints of the $\mathrm{MINLP}_{\mathrm{Design}}$ Model and Parameter Values Used in Case Study

Model Constraint		Parameter Values Used in Case Study
Product mass		
$M_0 = \mathrm{Titer} \cdot \alpha \cdot V^{\mathrm{bior}}$	(A.1)	$\alpha = 75\%$
$M_s = \mathrm{Yd}_s \cdot M_{s-1}, \quad \forall s$	(A.2)	$\mathrm{Yd}_{\mathrm{hc}} = 95\%$, $\mathrm{Yd}_{\mathrm{vi}} = 90\%$, $\mathrm{Yd}_{\mathrm{vf}} = 95\%$, $\mathrm{Yd}_{\mathrm{ufdf}} = 90\%$, $\mathrm{Yd}_{\mathrm{bf}} = 98\%$, See Table 1 for s=aff, cex, aex values
Annual product output		
$\mathrm{Annu}O = \sigma \cdot N^{\mathrm{batch}} \cdot M_s, \quad \forall s = \mathrm{bf}$	(A.3)	$\sigma = 90\%$

TABLE A.1. *Continued*

Model Constraint		Parameter Values Used in Case Study
$N^{\text{batch}} \leq \text{Max}N^{\text{batch}}$	(A.4)	
Product volume		
$V_0^{\text{prod}} = \alpha \cdot V^{\text{bior}}$	(A.5)	$\alpha = 75\%$
$V_s^{\text{prod}} = (\text{Flu}V_s + 1) \cdot V_0^{\text{prod}}, \quad \forall s = h$	(A.6)	$\text{Flu}V_{\text{hc}} = 0.1$
$V_s^{\text{prod}} = \text{EluCV}_s \cdot N_s^{\text{cyc}} \cdot \text{Tot}V_s^{\text{col}}, \quad \forall s = \text{aff, cex}$	(A.7)	See Table 1 for EluCV_s values
$V_s^{\text{prod}} = V_{s-1}^{\text{prod}}, \quad \forall s = \text{aex}$	(A.8)	
$V_s^{\text{prod}} = (\text{Neu}V_s + 1) \cdot V_{s-1}^{\text{prod}}, \quad \forall s = \text{vi}$	(A.9)	$\text{Neu}V_{\text{vi}} = 1.75$
$V_s^{\text{prod}} = (\text{Flu}V_s + 1) \cdot V_{s-1}^{\text{prod}}, \quad \forall s = \text{vf}$	(A.10)	$\text{Flu}V_{\text{vf}} = 0.3$
$V_s^{\text{prod}} = \frac{M_s}{F\text{Conc}}, \quad \forall s = \text{ufdf}$	(A.11)	$F\text{Conc} = 75 \ \text{mg/mL}$
Chromatography resin volume		
$\text{Tot}V_s^{\text{col}} = \sum_i N_{si}^{\text{col}} \cdot V_{si}^{\text{col}}, \quad \forall s \in \text{CS}$	(A.12)	
$\sum_i X_{si}^{\text{col}} = 1, \quad \forall s \in \text{CS}$	(A.13)	
$N_s^{\text{cyc}} \cdot \text{Tot}V_s^{\text{col}} \geq \text{Min}V_s^{\text{resin}}, \quad \forall s \in \text{CS}$	(A.14)	
$\text{Min}V_s^{\text{resin}} = \frac{M_{s-1}}{\text{DBC}_s \cdot \mu}, \quad \forall s \in \text{CS}$	(A.15)	$\mu = 95\%$, see Table 1 for DBC_s values
$N_s^{\text{cyc}} \leq \text{Max}N_s^{\text{cyc}}, \quad \forall s \in \text{CS}$	(A.16)	$\text{Max}N_s^{\text{cyc}} = 10$
Buffer usage		
$V_s^{\text{buff}} = \text{Flu}V_s \cdot V_0^{\text{prod}}, \quad \forall s = h$	(A.17)	$\text{Flu}V_{\text{hc}} = 0.1$
$V_s^{\text{buff}} = \text{BuffCV}_s \cdot N_s^{\text{cyc}} \cdot \text{Tot}V_s^{\text{col}}, \quad \forall s \in \text{CS}$	(A.18)	See Table 1 for BuffCV_s values
$V_s^{\text{buff}} = \text{Neu}V_s \cdot V_{s-1}^{\text{prod}}, \quad \forall s = \text{vi}$	(A.19)	$\text{Neu}V_{\text{vi}} = 1.75$
$V_s^{\text{buff}} = \text{Flu}V_s \cdot V_{s-1}^{\text{prod}}, \quad \forall s = \text{vf}$	(A.20)	$\text{Flu}V_{\text{vf}} = 0.3$
$V_s^{\text{buff}} = \text{DFV} \cdot \frac{M_s}{F\text{Conc}}, \quad \forall s = \text{ufdf}$	(A.21)	$\text{DFV} = 7, \ F\text{Conc} = 75 \ \text{mg/mL}$
$\text{Annu}V^{\text{buff}} = N^{\text{batch}} \cdot \sum_s V_s^{\text{buff}}$	(A.22)	
Processing time		
$T_s^{\text{dsp}} = T_s^{\text{prod}} + T_s^{\text{buff}}, \quad \forall s \in \text{CS}$	(A.23)	
$T_s^{\text{prod}} = \frac{V_{s-1}^{\text{prod}}}{\text{VFR}_s \cdot \sum_i N_{si}^{\text{col}}}, \quad \forall s \in \text{CS}$	(A.24)	
$\text{VFR}_s = \left(\text{Vel}_s \cdot \pi \cdot \sum_i \left(\frac{\text{DM}_{si}^{\text{col}}}{2} \right)^2 \cdot X_{si} \right) / 1,000, \quad \forall s \in \text{CS}$	(A.25)	See Table 1 for Vel_s values
$T_s^{\text{buff}} = \frac{V_s^{\text{buff}}}{\text{VFR}_s}, \quad \forall s \in \text{CS}$	(A.26)	
$\text{Batch}T^{\text{dsp}} = \frac{\sum_s T_s^{\text{dsp}}}{N_{\text{shift}}^{\text{hour}} \cdot N^{\text{shift}}}$	(A.27)	$N_{\text{shift}}^{\text{hour}} = 8, N^{\text{shift}} = 1$ $T_{\text{hc}}^{\text{dsp}} = T_{\text{vf}}^{\text{dsp}} = T_{\text{ufdf}}^{\text{dsp}} = 4, T_{\text{vi}}^{\text{dsp}} = 1.5, \ T_{\text{bf}}^{\text{dsp}} = 6$
$\text{Annu}T^{\text{dsp}} = N^{\text{batch}} \cdot \text{Batch}T^{\text{dsp}}$	(A.28)	
$\text{Annu}T^{\text{dsp}} \leq T^{\text{annu}} - T^{\text{bior}}$	(A.29)	$T^{\text{annu}} = 340, \ T^{\text{bior}} = 15$
Materials cost		
$C^{\text{resin}} = \sum_{s \in \text{CS}} \frac{A \cdot \text{Pc}_s^{\text{resin}} \cdot N^{\text{batch}} \cdot N_s^{\text{cyc}} \cdot \text{Tot}V_s^{\text{col}}}{L}$	(A.30)	$A = 1.1, L = 100$ see Table 1 for $\text{Pc}_s^{\text{resin}}$ values
$C^{\text{buff}} = \text{Pc}^{\text{buff}} \cdot \text{Annu}V^{\text{buff}}$	(A.31)	$\text{Pc}^{\text{buff}} = 1 \ £/L$
$C^{\text{media}} = \theta \cdot N^{\text{batch}} \cdot \text{Pc}^{\text{media}} \cdot \alpha \cdot V^{\text{bior}}$	(A.32)	$\theta = 1.2, \ \alpha = 0.75, \ \text{Pc}^{\text{media}} = 32 \ £/L$
$C^{\text{materials}} = \left(1 + \lambda^{\text{misc}} \right) \cdot \left(C^{\text{resin}} + C^{\text{buff}} + C^{\text{media}} \right)$	(A.33)	$\lambda^{\text{misc}} = 0.1$
Labor cost		
$C^{\text{directlab}} = W \cdot N^{\text{batch}} \cdot \left(N^{\text{operU}} \cdot T^{\text{bior}} \cdot 24 + \ N^{\text{operD}} \cdot \text{Batch}T^{\text{dsp}} \cdot N_{\text{shift}}^{\text{hour}} \cdot N^{\text{shift}} \right)$ $N_{\text{shift}}^{\text{hour}} = 8, N^{\text{shift}} = 1$	(A.34)	$W = 20 \ £/h, \ N^{\text{operU}} = 3, N^{\text{operD}} = 15,$
$C^{\text{labor}} = (1 + \lambda^{\text{othlabor}}) . C^{\text{directlab}}$	(A.35)	$\lambda^{\text{othlabour}} = 2.2$
Utilities cost		
$C^{\text{utilities}} = a \cdot N^{\text{bior}} \cdot V^{\text{bior}} + b \cdot N^{\text{batch}} \cdot V^{\text{bior}} + c \cdot \text{Annu}V^{\text{buff}}$	(A.36)	$a = 14.1 \ £/\text{L}, \ b = 4.2 \ £/\text{L}, \ c = 0.07 \ £/\text{L}$
Capital cost		
$C_{si}^{\text{col}} = \text{Ref}C^{\text{col}} \cdot \left(\frac{\text{DM}_{si}^{\text{col}}}{\text{RefDM}^{\text{col}}} \right)^{\text{SUF}^{\text{col}}}$	(A.37)	$\text{Ref}C^{\text{col}} = 170\text{k} \ £, \ \cdot\text{RefDM}^{\text{col}} = 100 \ \text{cm}, \ \text{SUF}^{\text{col}} = 0.8$
$C^{\text{bior}} = \text{Ref}C^{\text{bior}} \cdot \left(\frac{V^{\text{bior}}}{\text{Ref}V^{\text{bior}}} \right)^{\text{SUF}^{\text{bior}}}$	(A.38)	$\text{Ref}C^{\text{bior}} = 612\text{k} \ £, \ \cdot\text{Ref}V^{\text{bior}} = 2000 \ \text{L}, \ \text{SUF}^{\text{bior}} = 0.6$
$C^{\text{capital}} = \text{FCI} \cdot \frac{r \cdot (1+r)^{\text{ny}}}{(1+r)^{\text{ny}} - 1}$	(A.39)	$r = 10\%, \ \text{ny} = 10$
$\text{FCI} = \text{Lang}F \cdot (1 + \text{GEF}) \cdot \left(N^{\text{bior}} \cdot C^{\text{bior}} + \sum_{s \in \text{CS}} \sum_i N_{si}^{\text{col}} \cdot C_{si}^{\text{col}} + \lambda^{\text{otheq}} \cdot N^{\text{bior}} \cdot C^{\text{bior}} \right)$	(A.40)	$\text{Lang}F = 6, \ \cdot\text{GEF} = 0.7, \ \lambda^{\text{othequip}} = 0.8$
Other indirect costs		
$C^{\text{othindirect}} = \text{FCI} \cdot \lambda^{\text{othindirect}} + \text{GU} \cdot N^{\text{bior}} \cdot V^{\text{bior}}$	(A.41)	$\lambda^{\text{othindirect}} = 0065, \ \text{GU} = 90 \ £/\text{L}$
Total annual cost		
$\text{Annu}C = C^{\text{labout}} + C^{\text{materials}} + C^{\text{utilities}} + C^{\text{capital}} + C^{\text{othindirect}}$	(A.42)	

Manuscript received May 28, 2013, and revision received Aug. 10, 2013.